

Human MD2 deficiency – an inborn error of immunity with pleiotropic features

Yue Li, MSc ^{1*}, Ziqi Yu, MSc ^{1*}, Madlin Schenk, MSc ¹, Irena Lagovsky, MD PhD ², David Illig, PhD ¹, Christoph Walz, MD PhD ³, Meino Rohlf, PhD ¹, Raffaele Conca¹, Aleixo M. Muise, MD PhD ^{4,5,6,7,16}, Scott B. Snapper, MD PhD ^{8,9,10,16}, Holm H. Uhlig, MD PhD ^{11,16}, Ben Zion Garty, MD PhD ^{12,13}, Christoph Klein, MD PhD ^{1,14,15,16}, Daniel Kotlarz, MD PhD ^{1,16,17#}

¹Dr. von Hauner Children's Hospital, Department of Pediatrics, University Hospital, Ludwig-Maximilians-Universität (LMU) Munich, 80337 Munich, Germany; ²Felsenstein Medical Research Center, Rabin Medical Center and Sackler School of Medicine Tel Aviv, Israel; ³Institute of Pathology, Faculty of Medicine, LMU Munich, 80336 Munich, Germany; ⁴SickKids Inflammatory Bowel Disease Center, Research Institute, Hospital for Sick Children, Toronto, ON M5G1X8 Canada; ⁵Cell Biology Program, Research Institute, Hospital for Sick Children, Toronto, ON M5G1X8 Canada; ⁶Division of Gastroenterology, Hepatology and Nutrition, Department of Pediatrics, Hospital for Sick Children, University of Toronto, Toronto, ON M5G1X8 Canada; ⁷Department of Biochemistry, University of Toronto, Toronto, ON M5G1A8 Canada; ⁸Division of Gastroenterology, Hepatology and Nutrition, Boston Children's Hospital, Boston, MA 02115 USA; ⁹Department of Medicine, Harvard Medical School, Boston, MA 02115 USA; ¹⁰Division of Gastroenterology, Brigham and Women's Hospital, Boston, MA 02115 USA; ¹¹Translational Gastroenterology Unit and Department of Pediatrics, and Biomedical Research Centre, University of Oxford, Oxford, UK; ¹²Sackler School of Medicine, Tel Aviv University, Tel-Aviv, Israel; ¹³Allergy and Clinical Immunology Unit, Schneider Children's Medical Center, Petach-Tikva, Israel; ¹⁴Gene Center, LMU Munich, Munich, Germany; ¹⁵Deutsche Zentrum für Infektionsforschung (DZIF) and Deutsches Zentrum für Kinder- und Jugendgesundheit, partner site Munich, Germany; ¹⁶VEO-IBD Consortium; ¹⁷Institute of Translational Genomics, Helmholtz Zentrum München - German Research Center for Environmental Health, Ingolstädter Landstraße 1, 85764 Neuherberg, Germany. *Contributed equally. #Corresponding author: Daniel Kotlarz, Email: daniel.kotlarz@med.uni-muenchen.de

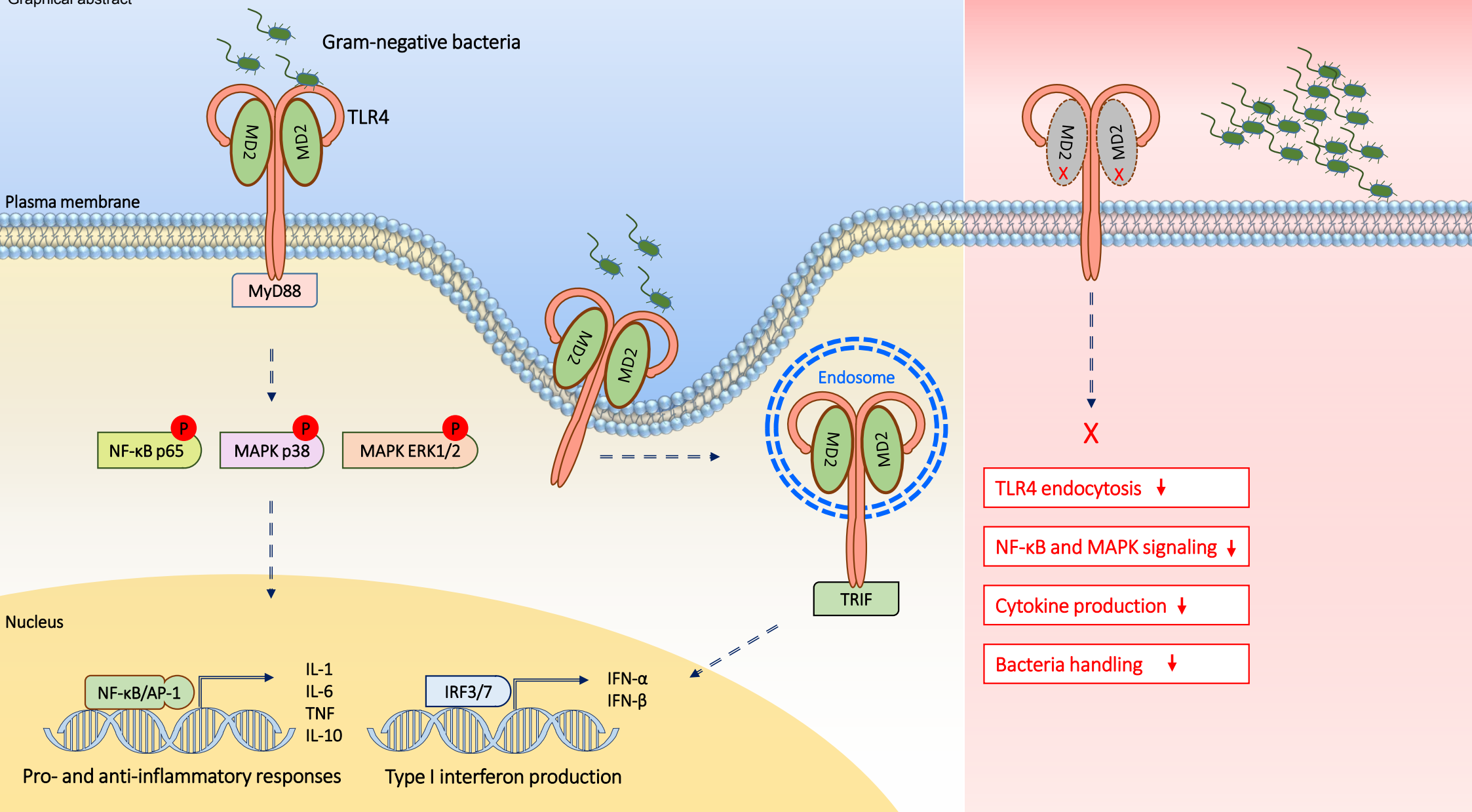
Capsule Summary: Biallelic MD2 deficiency causes abrogated TLR4-dependent inflammatory responses to gram-negative bacteria with variable expressivity

Running title: Human MD2 deficiency.

Key words: MD2/TLR4, inborn error of immunity, inflammatory bowel disease, pediatrics, genomics, host-pathogen interactions

Abbreviation: TLR: toll-like receptors, MD2: myeloid differentiation protein 2, LPS: lipopolysaccharide, VEO-IBD: very early onset inflammatory bowel disease, KO: knockout, PRR: pathogen recognition receptor, LBP: LPS-binding protein, MyD88: myeloid differentiation primary response 88, TRIF: TIR-domain-containing adaptor-inducing IFN- β , HMGB1: high mobility group box 1, IRAK4: interleukin-1 receptor-associated kinase 4. WES: whole exome sequencing, EBV-LCL: EBV-transformed lymphoblastoid cell lines, KI: knockin, iPSC: induced pluripotent stem cells, EEA1: early endosomal antigen 1, TIRAP: toll-interleukin 1 receptor domain containing adaptor protein

Graphical abstract



Abstract

Background: Toll-like receptors (TLRs) are important pattern recognition receptors that sense microbes and control host defense. Myeloid differentiation protein 2 (MD2) is the indispensable co-receptor for TLR4 facilitating the binding to the gram-negative bacterial cell wall component lipopolysaccharide (LPS) and activation of downstream signaling.

Objective: To provide phenotypic and mechanistic insights on human MD2 deficiency.

Methods: To elucidate the genetic cause in a patient with very early onset inflammatory bowel disease (VEO-IBD), we performed whole exome sequencing and studied the functional consequences of the identified mutation in *LY96* (encoding for MD2) in genetically engineered iPSC-derived macrophages with knockout (KO) of MD2 or knockin of the patient-specific mutation, including TLR4-mediated signaling, cytokine production and bacterial handling.

Results: WES identified a homozygous in-frame deletion in the *LY96* gene (c.347_349delCAA; p.Thr116del) in a patient with VEO-IBD and a sibling presenting with pneumonia and otitis media. iPSC-derived macrophages with KO of MD2 or expression of the Thr116del mutation showed impaired activation of NF- κ B and MAPK signaling as well as TLR4 endocytosis upon challenge with LPS or bacteria. In addition, MD2-deficient macrophages showed decreased cytokine expression (e.g., IL6, TNF and IL10) in response to LPS or gram-negative but not gram-positive bacteria.

Conclusion: Human MD2 deficiency causes defective TLR4 signaling in response to LPS or gram-negative bacteria. The clinical manifestations and expressivity might be variable due to unknown secondary risk factors. Since TLR4 represents a therapeutic target for multiple inflammatory conditions, our study may provide insights into potential side effects by pharmacological TLR4 targeting.

Introduction

An intricate balance of host-pathogen interactions is critical in controlling tissue homeostasis. Microbial pathogens can be sensed by innate immune cells through a wide range of pattern recognition receptors (PRRs) such as the family of toll-like receptors (TLRs) (1). For example, TLR4 is crucial for the recognition of lipopolysaccharide (LPS) from gram-negative bacterial cell walls. Upon LPS sensitization by the two accessory proteins, LPS-binding protein (LBP) and CD14, monomeric LPS will be transferred to heterodimers comprising of myeloid differentiation protein 2 (MD2) and TLR4 (2). MD2 represents an essential co-receptor required for LPS recognition and TLR4 activation by inducing the aggregation of the TLR4-MD2 multimeric complex and selecting TLR4 as cargo for endocytosis (2, 3). In response to TLR4-MD2 engagement, activation of proinflammatory signaling will be induced by the recruitment of the adaptor proteins myeloid differentiation primary response 88 (MyD88) (4) and TIR-domain-containing adaptor-inducing IFN- β (TRIF) (5). In addition to LPS-induced TLR4 signaling, MD-2 has been shown to mediate TLR2-dependent inflammatory responses to LPS (6) and disulfide high mobility group box 1 (HMGB1)-mediated activation of TLR4 (7). TLR4/MyD88 signaling has been implicated in several inflammatory conditions such as inflammatory bowel disease (IBD), lupus-like autoimmune disease, sepsis, and cardiovascular diseases (8). As the gastrointestinal tract contains the largest numbers of bacteria, imbalances of the microbiome or altered sensing of microorganisms could result in inappropriate immune responses. In mouse models, the role of TLR4 signaling in intestinal pathology remains controversial. Whereas constitutive knockout of *Tlr4* results in increased mortality and intestinal epithelial injury (9, 10), mice with transgenic expression of constitutive activate TLR4 in the intestinal epithelium showed augmented colitis (11). Based on these studies, intestinal TLR4 signaling controls both proinflammatory response and immune tolerance. In human, several studies have associated TLR4 polymorphisms with IBD and deficiencies in the TLR-downstream proteins MyD88 or interleukin-1 receptor-associated kinase 4 (IRAK4) lead

99 to human inborn errors of immunity with increased susceptibility to infections by pyogenic
100 bacteria (12, 13). Despite the critical role of TLR4 signaling in innate immunity and intestinal
101 homeostasis, no patients with TLR4 or MD2 deficiency have yet been reported.

Results and Discussion

Our index patient (A.II-1) presented with infantile colitis associated with failure-to-thrive, bloody diarrhea and perianal abscesses since the age of 4 months (Fig. 1A). Colonoscopy revealed pancolitis with mucosal erosions and hemorrhages (Fig. 1B). Histological examination confirmed moderately chronic and mildly active ileocolitis accompanied by fissural ulcerations, epithelial regeneration, mucosal hemorrhage, crypt abscesses, and crypt distortion (Fig. 1C, suppl Fig. S1A). Furthermore, he developed bronchiectasis and persistent pneumonia that required lobectomy of the left lower lobe and the lingula at the age of 6 years. Despite state-of-the-art immunosuppressive and anti-inflammatory treatment (e.g., steroids, azathioprine, methotrexate, infliximab, adalimumab, cyclosporine and vedolizumab) he showed a refractory colitis and had to undergo colectomy and ileostomy at the age of 12 years. Currently, he shows a stable disease course at the age of 18 years.

To elucidate potential genetic causes for VEO-IBD, we have performed whole exome sequencing (WES). Our genetic screen revealed a 3 bp homozygous in frame deletion in the *LY96* gene (NM_015364.5, c.347_349delCAA; p.Thr116del) in A.II-1 (P1) following an autosomal recessive inheritance pattern, as both parents were heterozygous for the mutation (Fig. 1A). Notably, the *LY96* deletion could be also detected in the brother A.II-5 who presented with recurrent otitis media and pneumonia but exhibited no signs of intestinal inflammation at the age of 11 years. All other available healthy siblings had a wildtype (WT) genotype or were heterozygous for the mutation, as determined by Sanger sequencing (Fig. 1A).

To evaluate the impact of the mutation on gene expression, we assessed *LY96* RNA level in EBV-transformed lymphoblastoid cell lines (EBV-LCL). RT-PCR data showed comparable expression of *LY96* among patient A.II-1, father, and healthy donors (suppl Fig. S1B).

Previous studies have suggested that the N-linked glycosylation at position Asn114 is critical for the secretion and stability of MD2 (14). In view of the close proximity, it was suggestive that the Thr116del mutation might disturb the consensus sequence (Asn-x-Ser/Thr/Cys) for

N-glycosylation and affect MD2 secretion (Fig. 1D). To evaluate the impact of the mutation on protein expression, we overexpressed C-terminal flag-tagged WT and mutant MD2 in HEK293T cells. Immunoblotting revealed a reduced molecular weight of the Thr116del mutant in comparison to WT MD2. To assess whether the difference in molecular weight between WT and mutant MD2 is caused by an impaired N-linked glycosylation, we treated the cell lysates with the N-glycosidases. Upon exposure to both Endo H or PNGase F we could observe comparable mobility of the deglycosylated WT and mutant MD2 variants, suggesting defective N-linked glycosylation of mutant MD2 (Fig. 1E).

It is well known that TLR4 is essential for LPS-mediated NF- κ B signaling and subsequent cellular activation (15). To assess the functional relevance of the mutation in MD2 on TLR4-induced signaling, we have generated a CRISPR/Cas9-mediated knockout (KO) of MD2 or knockin (KI) of the patient-specific mutation p.Thr116del in WT induced pluripotent stem cells (iPSCs). In a first setting, we assessed the TLR4-mediated downstream signaling in iPSC-derived macrophages upon stimulation with LPS. Immunoblotting revealed reduced phosphorylation of NF- κ B p65 (Ser536), ERK1/2 (Thr202/Tyr204), and p38 MAPK (Thr180/Tyr182) in macrophages with KO of *LY96* and KI of the mutation Thr116del (Fig. 2A). As a consequence of impaired TLR4-mediated NF- κ B activation, we could detect a reduced IL-1 β production and secretion in patient-derived monocytes (Fig. 2B) and MD2-deficient iPSC-derived macrophages (KO or KI) upon inflammasome activation by treatment with LPS and nigericin (Fig. 2C, Suppl Fig. S2). In addition, we could detect a decreased LPS-induced expression of other proinflammatory cytokines (e.g., TNF and IL-6) in MD2-deficient macrophages (Fig. 2D). Previous studies have shown that MD2 is required for the TLR4 activation and is a cargo-selecting agent for endocytosis of TLR4 (3). Correspondingly, our flow cytometry data indicated impaired internalization of surface TLR4 upon challenge with LPS in iPSC-derived macrophages with KO of MD2 or KI of the Thr116del mutation (Fig. 2E). Furthermore, confocal microscopic analysis showed less TLR4 colocalization with early

endosomal antigen 1 (EEA1) in MD2-deficient macrophages over time compared to WT macrophages (Fig. 2F).

Gastrointestinal pathogens have been implicated as environmental triggers in IBD (16). For example, enteropathogenic *Escherichia coli* and *Salmonella typhimurium* are known diarrhea-causing gram-negative bacteria (17). Efficient recognition of these pathogens by PRRs is crucial for proper activation of inflammatory mediators. To assess whether MD2 deficiency could result in defective bacterial handling and compromised innate immune responses caused by enteropathogenic bacteria, we infected MD2-deficient macrophages with *E. coli*. Immunoblotting suggested a reduced activation of NF- κ B and MAPK signaling in cells with mutant MD2 (Fig. 3A). Furthermore, *E. coli* infection failed to induce robust inflammasome activation in MD2-deficient macrophages, as indicated by reduced IL-1 β secretion measured by ELISA and immunoblotting (Fig. 3B). In line with defective TLR4 internalization and endocytosis, flow cytometry analysis showed persistent cell surface TLR4 staining in MD2-deficient macrophages compared to WT cells upon bacterial exposure (Fig. 3C). To assess the bacterial handling, we challenged MD2-deficient macrophages with *Salmonella typhimurium* in gentamycin protection assays. Reduced colony formation derived from intracellular bacteria could be detected in MD2-deficient macrophages, indicating impaired phagocytosis or enhanced bacterial killing (Suppl Fig. S3A). Since we could not detect increased LC3B or lysotracker staining in MD2-deficient macrophages, our data suggest that the differences in the colony formation are rather not associated with enhanced bacterial killing (Fig. 3D). Next, we performed live cell imaging to track the phagocytosis using pHrodo Red *E. coli* bioparticles, which only show bright fluorescence in acidic compartment such as phagosomes. In comparison to WT cells, MD2-deficient macrophages showed a delayed kinetics and overall reduction of phagocytosis (Fig. 3E). To investigate whether the MD2 deficiency has specific effects on gram-negative bacteria, we compared the cytokine responses of WT and MD2-

deficient macrophages upon exposure to *E. coli* or *Salmonella typhimurium* in comparison to gram-positive *Listeria monocytogenes*. RT-PCR analysis showed impaired MyD88- and TRIF-dependent cytokine production (*IL6*, *TNF*, *IL10*, *IFNB*) in MD2-deficient macrophages upon infection with both *E. coli* and *Salmonella typhimurium*, whereas the *Listeria monocytogenes*-induced cytokine responses were comparable with WT cells (Fig. 3F).

The consequence of defective TLR4/MD2 signaling has previously not been characterized in human physiological settings. Here, we report a biallelic 3 bp in-frame deletion in *LY96* in a patient suffering from VEO-IBD and a sibling presenting with pneumonia and recurrent otitis media. Our experimental studies on genetically engineered iPSCs with KO of MD2 or KI of the patient-specific mutation showed that biallelic MD2 deficiency leads to impaired TLR4-mediated signalling, cytokine responses, and bacterial handling.

IBD is a chronic and relapsing condition in the gastrointestinal tract that can be triggered by multiple factors such as genetic susceptibility, immune dysregulation, environmental risks and microbiome imbalance. In particular, abnormal intestinal immune responses to gut flora are considered as risk for IBD pathogenesis (18). Several studies have demonstrated that *Tlr2*^{-/-}, *Tlr4*^{-/-}, and *MyD88*^{-/-} mice exhibit increased mortality and colonic injury upon treatment with DSS (19, 20). Furthermore, administration of LPS has been shown to increase the survival rate in experimental colitis models, suggesting that recognition of commensal bacteria by TLRs is protective to colonic injury (10). Moreover, human MyD88 and IRAK4 deficiencies are known to cause severe TLR- and IL-1-mediated inborn errors of immunity with increased susceptibility to pyogenic bacteria (12, 13). In addition, biallelic toll-interleukin 1 receptor domain containing adaptor protein (TIRAP) deficiency was also reported to cause life-threatening staphylococcal disease with incomplete penetrance (21). In parallel studies, Capitani et al. report a patient with TLR4 deficiency presenting with complex perianal Crohn's disease and wound healing problems similar to our index patient. As both studies confirmed

204 defective TLR4-dependent signaling in innate immune cells upon exposure to bacterial
205 antigens, one might consider targeting of IBD-associated gut microbiota by antibiotics or
206 allogenic hematopoietic stem cell transplantation as treatment option. However, MD2 and
207 TLR4 deficiencies were associated with variable expressivity, incomplete penetrance and/or
208 variant segregation. The variability in disease onset and manifestation might be due to exposure
209 to other risk factors (e.g., bacterial infections, environmental triggers, genetic polymorphisms),
210 TLR4-dependent effects on non-hematopoietic cells, or compensatory mechanisms of other
211 TLRs in contrast to previously described IRAK4 and MYD88 deficiencies (8). Therefore,
212 further studies on larger patient cohorts of TLR4/MD2 deficiency are required to unveil the
213 molecular disease mechanisms and triggers and to evaluate the therapeutic implications. Even
214 though we cannot confirm a causal association of TLR4 and MD2 deficiencies with IBD or
215 primary immunodeficiency, our studies provide critical insights on human TLR4/MD2 biology.
216 Several studies have already implicated TLR4 in disease development and progression, and
217 inhibition of TLR4 has been proposed for the treatment of multiple inflammatory conditions
218 (e.g., IBD, septic shock, rheumatoid arthritis, cardiovascular diseases) (8). However, our studies
219 warrant caution on therapeutics strategies targeting TLR4 signaling.

Acknowledgment

We dedicate our study to the affected patients. We acknowledge the help from the Care-for-Rare Genomics Core Facility and the Flow Cytometry Core Facility at the Dr. von Hauner Children's Hospital. We are grateful for the involved interdisciplinary medical teams. We thank Helmholtz Center Munich for providing the HMGU1 iPSCs, Addgene for granting the plasmid px458, and Dr. Felipe Romero for supplying the *E.coli. Salmonella enterica serovar typhimurium* (*S. typhimurium*)-expressing GFP was kindly provided by David Holden (Imperial College, University of London, UK). This work has been supported by Leona M. and Harry B. Helmsley Charitable Trust, DFG (Gottfried-Wilhelm-Leibniz Program, Heinz Maier-Leibnitz-Preis, Collaborative Research Consortium SFB1054 project A05), PID-NET (BMBF), and the Care-for-Rare Foundation. Z.Y. is supported by the China Scholarship Council. Y.L. has received the Care-for-Rare scholarship. Daniel Kotlarz has been a scholar funded by the Daimler und Benz Stiftung, Reinhard-Frank Stiftung, and Else-Kröner-Fresenius Stiftung. The Authors declare no conflict of interest.

Author contribution

Y.L. and Z.Y. performed the experiment and analysed the data. M. S. performed Sanger sequencing and generated the CRISPR/Cas9-mediated KO and KI iPSCs. D.I. optimized the protocol for macrophage differentiation. B.Z.G. and I.L. are the referring physicians of the index patient and provided clinical information. C.W. performed histological analysis. M.R. performed genome sequencing. R.C. conducted immunophenotyping. A.M., S.S., H.U. were critical in the interpretation of the human data. Y.L. and D.K. wrote the manuscript. C.K. and D.K. conceived the study design, and supervised Y.L., Z.Y., M.S., and D.I.. All authors interpreted the data and approved the final version of the manuscript.

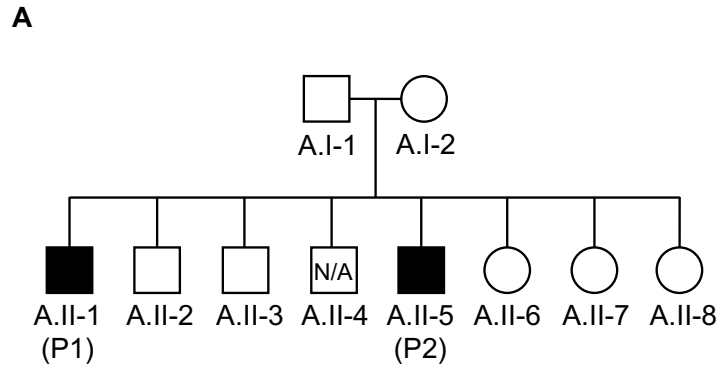
Figure Legends

Figure 1. (A) Sanger sequencing confirmed the homozygous mutation in index patient (A.II- 1) and one of the sibling (A.II-5). (B) Colonoscopy revealed pancolitis with mucosal erosions. (C) Overview magnification displays broad areas of erosion and fissural ulceration (arrow), mucosal hemorrhage and crypt distortion (arrowhead). Scale bar is 1000 μ m (i). The inflammatory infiltrate is predominantly chronic and consists of plasma cells and lymphocytes with scattered eosinophilic and neutrophilic granulocytes representing a mild florid component. Few small crypt abscesses were also present (arrow). Scale bar is 100 μ m (ii). (D) Structural annotation of human MD2 (blue) with lipid IVa (10.2210/pdb2e59/pdb). Black arrow points to N-linked glycosylation on Asn114. Red arrow indicates the mutation position at Thr116. (E) Analysis of N-linked glycosylation on WT and mutant MD2. C-terminal flag-tagged WT and mutant MD2 were overexpressed in HEK293T cells. Cell lysates were treated with PNGase F and Endo H. Protein molecular weight was analyzed in SDS-PAGE before and after deglycosylation.

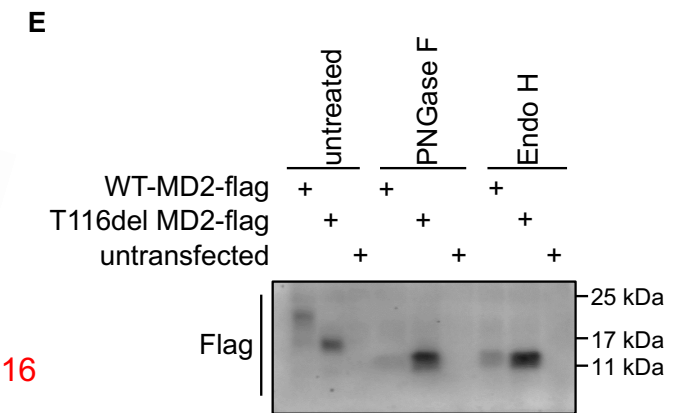
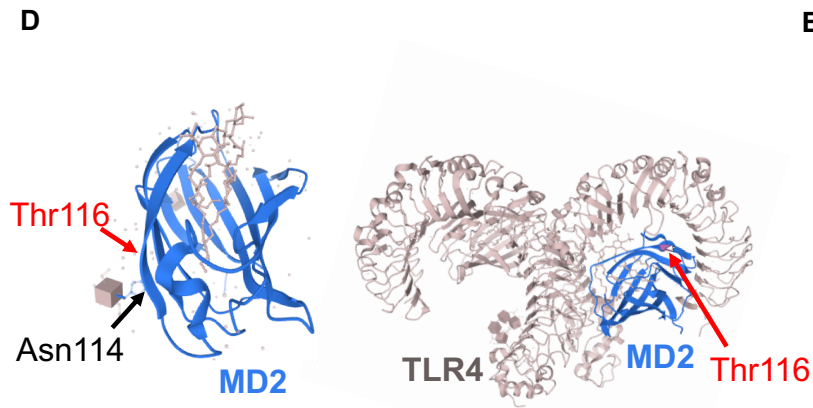
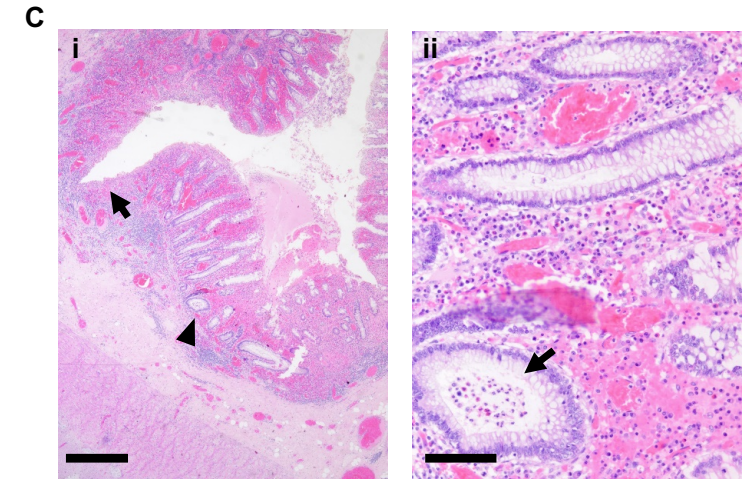
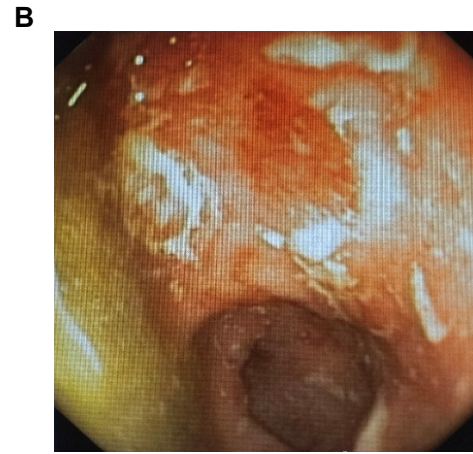
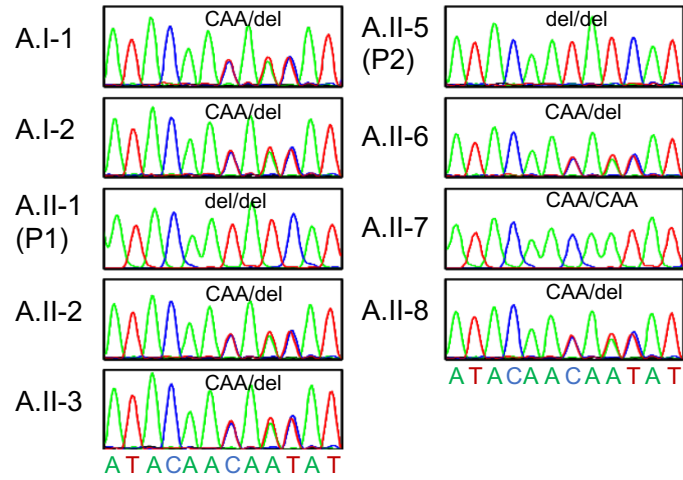
Figure 2. Functional analysis of iPSC-derived macrophages upon LPS stimulation. (A) Immunoblotting showed reduced LPS-mediated activation of NF- κ B and MAPK signaling in iPSC-derived macrophages with KO of MD2 or KI of mutation p.Thr116del. (B) ELISA showed decreased secretion of mature IL-1 β upon stimulation with LPS and nigericin in monocytes derived from the patient (A.II-1) and the sibling with the same mutation (A.II-5). (C) ELISA confirmed reduced secretion of IL-1 β upon stimulation with LPS and nigericin in iPSC-derived macrophages with KO of MD2 or KI of the mutation p.Thr116del. (D) ELISA and qPCR showed reduced production of TNF and IL-6 upon LPS stimulation in macrophages derived from MD2-deficient iPSC. (E) Flow cytometry analysis of cell surface TLR4 showed impaired internalization of TLR4 in MD2-deficient macrophages upon LPS challenge. (F) Confocal immunofluorescence microscopy suggested that upon LPS binding, MD2-deficient

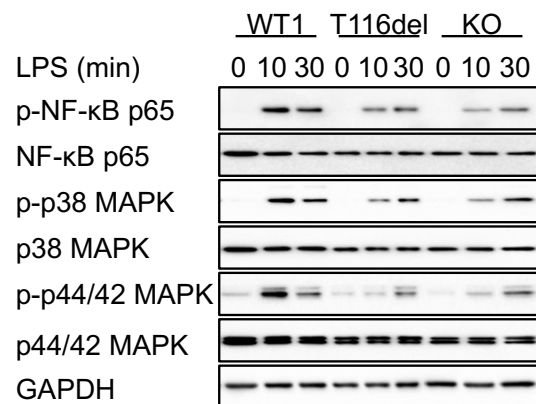
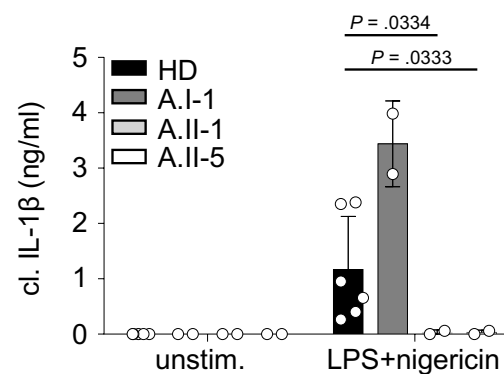
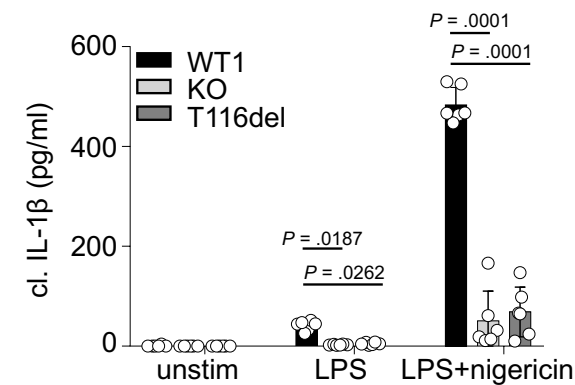
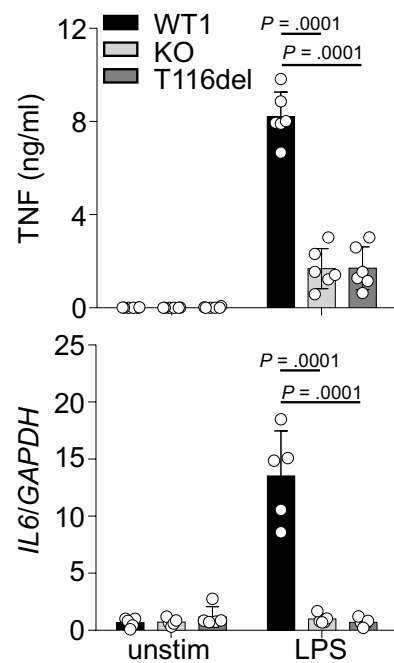
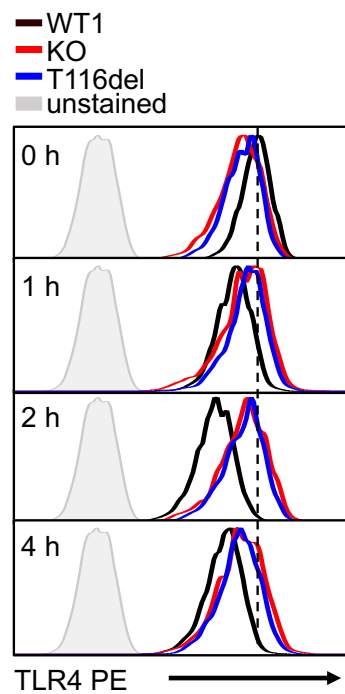
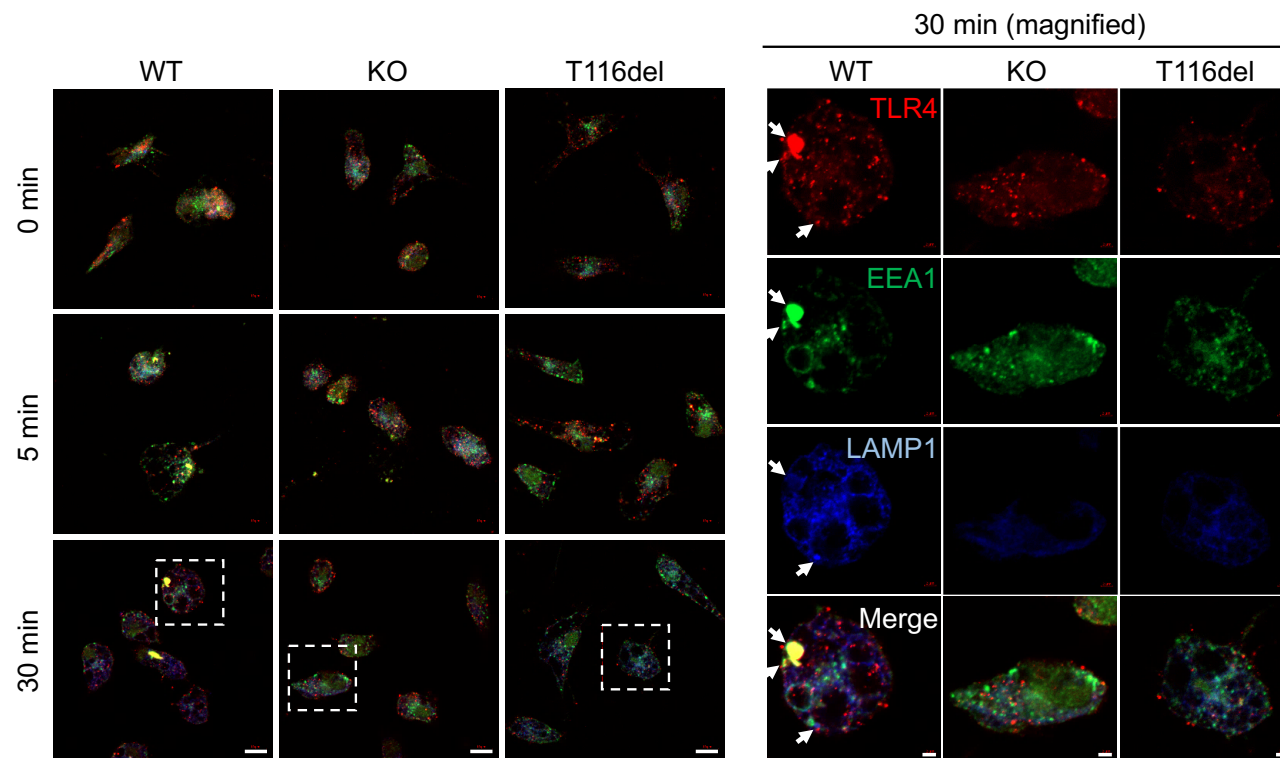
cells showed less co-localization of TLR4 (red) with endosome (EEA1, green) and lysosome (LAMP1, blue), indicated by arrows. Scale bar: left, 10 μ m; right, 2 μ m. The WT1 cells used throughout Figure 2 are from bulk culture of unmodified iPSCs.

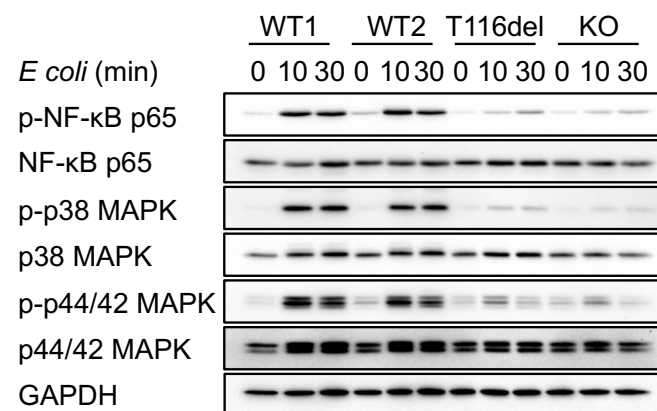
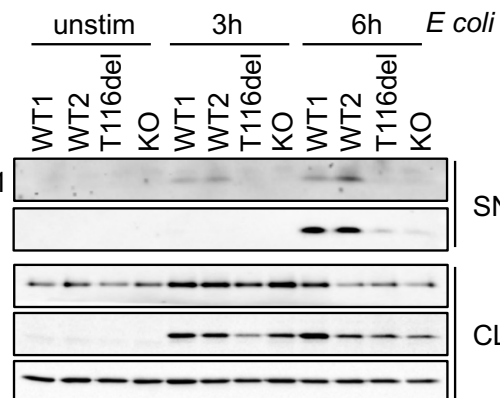
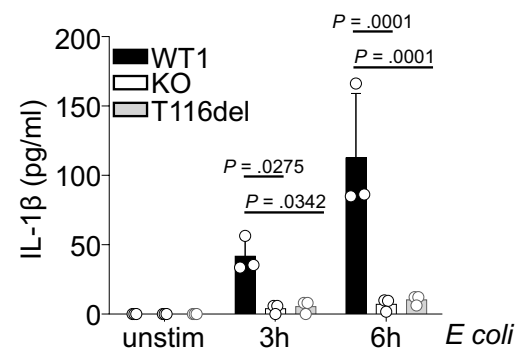
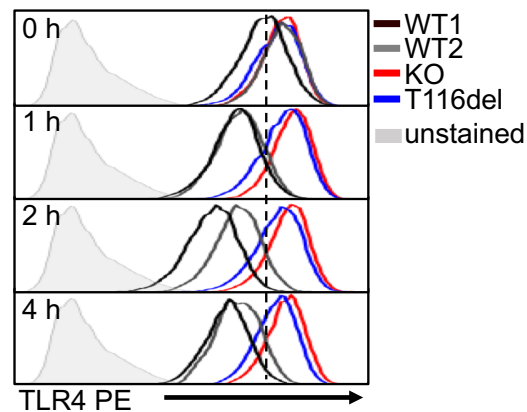
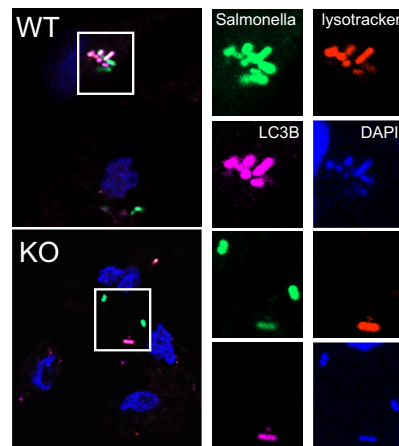
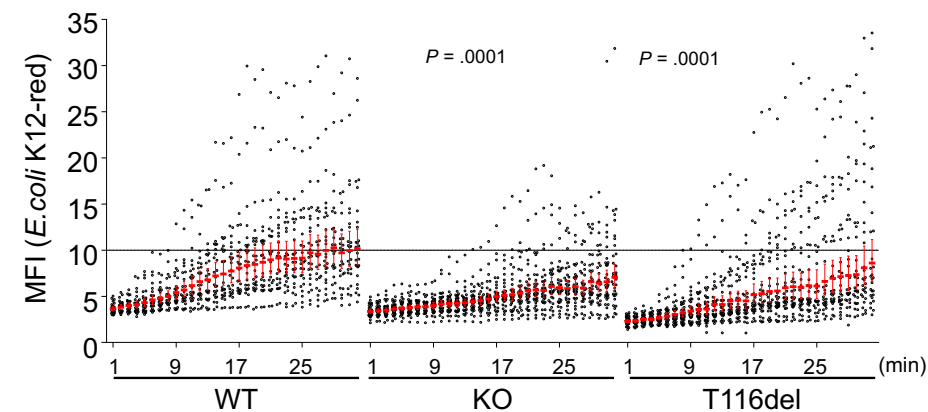
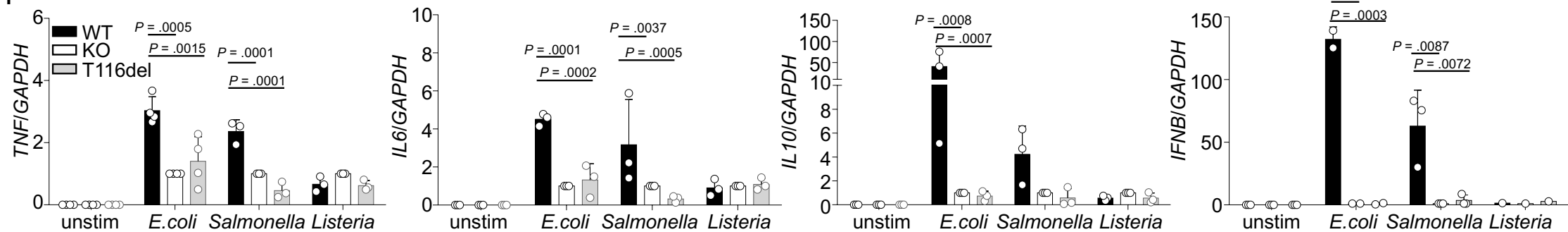
Figure 3. Functional analysis of iPSC-derived macrophages upon bacterial infection. **(A)** Immunoblotting showed impaired activation of NF- κ B and MAPK signaling upon *E.coli* infection. WT1 is from bulk culture of unmodified iPSCs. WT2 is unmodified single cell clone after CRISPR/Cas 9 treatment. **(B)** ELISA and immunoblotting showed reduced secretion of IL-1 β and caspase-1 upon *E.coli* infection in iPSC-derived macrophages with KO of MD2 and KI of the mutation p.Thr116del. WT1 (unmodified bulk culture) was used for ELISA, while both WT1 and WT2 (unmodified clone after CRISPR/Cas9 treatment) were used in immunoblotting. **(C)** Flow cytometry analysis of cell surface TLR4 showed impaired internalization of TLR4 in MD2-deficient macrophages upon infection with *E.coli*. **(D)** Confocal immunofluorescence analysis suggested normal phagosome-lysosome fusion in MD2 KO cells upon infection with *Salmonella typhimurium*. **(E)** Live cell imaging with pHrodo Red *E.coli* bioparticles suggested delayed phagocytosis. Mean fluorescence intensity was plotted according to median with 95% confidence interval for the duration of 32 minutes, each dot represents one cell. WT1 (unmodified bulk culture) was used in this assay. **(F)** Real-time qPCR showed reduced cytokine production in iPSC-derived macrophages with KO of MD2 and KI of the mutation p.Thr116del upon infection with *E.coli* and *Salmonella typhimurium*, but not with *Listeria monocytogenes*. WT1 (unmodified bulk culture) was used in these experiments.



c.347_349delCAA, p.Thr116del



A**B****C****D****E****F**

A**B****C****D****E****F**

293 **References**

- 294 1. Medzhitov R. Recognition of microorganisms and activation of the immune response.
295 Nature. 2007;449(7164):819-26.
- 296 2. Park BS, Song DH, Kim HM, Choi BS, Lee H, Lee JO. The structural basis of
297 lipopolysaccharide recognition by the TLR4-MD-2 complex. Nature. 2009;458(7242):1191-5.
- 298 3. Tan Y, Zanoni I, Cullen TW, Goodman AL, Kagan JC. Mechanisms of Toll-like Receptor
299 4 Endocytosis Reveal a Common Immune-Evasion Strategy Used by Pathogenic and
300 Commensal Bacteria. Immunity. 2015;43(5):909-22.
- 301 4. Piao W, Ru LW, Piepenbrink KH, Sundberg EJ, Vogel SN, Toshchakov VY. Recruitment
302 of TLR adapter TRIF to TLR4 signaling complex is mediated by the second helical region of
303 TRIF TIR domain. Proc Natl Acad Sci U S A. 2013;110(47):19036-41.
- 304 5. Yamamoto M, Sato S, Hemmi H, Hoshino K, Kaisho T, Sanjo H, et al. Role of adaptor
305 TRIF in the MyD88-independent toll-like receptor signaling pathway. Science.
306 2003;301(5633):640-3.
- 307 6. Dziarski R, Wang Q, Miyake K, Kirschning CJ, Gupta D. MD-2 enables Toll-like receptor
308 2 (TLR2)-mediated responses to lipopolysaccharide and enhances TLR2-mediated responses
309 to Gram-positive and Gram-negative bacteria and their cell wall components. J Immunol.
310 2001;166(3):1938-44.
- 311 7. Yang H, Wang H, Ju Z, Ragab AA, Lundback P, Long W, et al. MD-2 is required for
312 disulfide HMGB1-dependent TLR4 signaling. J Exp Med. 2015;212(1):5-14.
- 313 8. Gao W, Xiong Y, Li Q, Yang H. Inhibition of Toll-Like Receptor Signaling as a Promising
314 Therapy for Inflammatory Diseases: A Journey from Molecular to Nano Therapeutics. Front
315 Physiol. 2017;8:508.
- 316 9. Fukata M, Michelsen KS, Eri R, Thomas LS, Hu B, Lukasek K, et al. Toll-like receptor-4
317 is required for intestinal response to epithelial injury and limiting bacterial translocation in a
318 murine model of acute colitis. Am J Physiol Gastrointest Liver Physiol. 2005;288(5):G1055-
319 65.
- 320 10. Rakoff-Nahoum S, Paglino J, Eslami-Varzaneh F, Edberg S, Medzhitov R. Recognition
321 of commensal microflora by toll-like receptors is required for intestinal homeostasis. Cell.
322 2004;118(2):229-41.
- 323 11. Fukata M, Shang L, Santaolalla R, Sotolongo J, Pastorini C, Espana C, et al.
324 Constitutive activation of epithelial TLR4 augments inflammatory responses to mucosal
325 injury and drives colitis-associated tumorigenesis. Inflamm Bowel Dis. 2011;17(7):1464-73.
- 326 12. von Bernuth H, Picard C, Jin Z, Pankla R, Xiao H, Ku CL, et al. Pyogenic bacterial
327 infections in humans with MyD88 deficiency. Science. 2008;321(5889):691-6.
- 328 13. Picard C, Puel A, Bonnet M, Ku CL, Bustamante J, Yang K, et al. Pyogenic bacterial
329 infections in humans with IRAK-4 deficiency. Science. 2003;299(5615):2076-9.
- 330 14. Ohto U, Fukase K, Miyake K, Satow Y. Crystal structures of human MD-2 and its
331 complex with antiendotoxic lipid IVa. Science. 2007;316(5831):1632-4.
- 332 15. Chow JC, Young DW, Golenbock DT, Christ WJ, Gusovsky F. Toll-like receptor-4
333 mediates lipopolysaccharide-induced signal transduction. J Biol Chem. 1999;274(16):10689-
334 92.
- 335 16. Jostins L, Ripke S, Weersma RK, Duerr RH, McGovern DP, Hui KY, et al. Host-microbe
336 interactions have shaped the genetic architecture of inflammatory bowel disease. Nature.
337 2012;491(7422):119-24.
- 338 17. Reis RS, Horn F. Enteropathogenic Escherichia coli, Samonella, Shigella and Yersinia:
339 cellular aspects of host-bacteria interactions in enteric diseases. Gut Pathog. 2010;2(1):8.

- 340 18. Huang Y, Chen Z. Inflammatory bowel disease related innate immunity and adaptive
341 immunity. *Am J Transl Res*. 2016;8(6):2490-7.
- 342 19. Araki A, Kanai T, Ishikura T, Makita S, Uraushihara K, Iiyama R, et al. MyD88-deficient
343 mice develop severe intestinal inflammation in dextran sodium sulfate colitis. *J*
344 *Gastroenterol*. 2005;40(1):16-23.
- 345 20. Asquith MJ, Boulard O, Powrie F, Maloy KJ. Pathogenic and protective roles of MyD88
346 in leukocytes and epithelial cells in mouse models of inflammatory bowel disease.
347 *Gastroenterology*. 2010;139(2):519-29, 29 e1-2.
- 348 21. Israel L, Wang Y, Bulek K, Della Mina E, Zhang Z, Pedergnana V, et al. Human Adaptive
349 Immunity Rescues an Inborn Error of Innate Immunity. *Cell*. 2017;168(5):789-800 e10.
350

Human MD2 deficiency – an inborn error of immunity with pleiotropic features

Yue Li^{1*}, Ziqi Yu^{1*}, Madlin Schenk¹, Irena Lagovsky², David Illig¹, Christoph Walz³, Meino Rohlf¹, Raffaele Conca¹, Aleixo M. Muise^{4,5,6,7,16}, Scott B. Snapper^{8,9,10,16}, Holm H. Uhlig^{11,16}, Ben Zion Garty^{12,13}, Christoph Klein^{1,14,15,16}, Daniel Kotlarz^{1,16,17#}

¹Dr. von Hauner Children's Hospital, Department of Pediatrics, University Hospital, Ludwig-Maximilians-Universität (LMU) Munich, 80337 Munich, Germany; ²Felsenstein Medical Research Center, Rabin Medical Center and Sackler School of Medicine Tel Aviv, Israel; ³Institute of Pathology, Faculty of Medicine, LMU Munich, 80336 Munich, Germany; ⁴SickKids Inflammatory Bowel Disease Center, Research Institute, Hospital for Sick Children, Toronto, ON M5G1X8 Canada; ⁵Cell Biology Program, Research Institute, Hospital for Sick Children, Toronto, ON M5G1X8 Canada; ⁶Division of Gastroenterology, Hepatology and Nutrition, Department of Pediatrics, Hospital for Sick Children, University of Toronto, Toronto, ON M5G1X8 Canada; ⁷Department of Biochemistry, University of Toronto, Toronto, ON M5G1A8 Canada; ⁸Division of Gastroenterology, Hepatology and Nutrition, Boston Children's Hospital, Boston, MA 02115 USA; ⁹Department of Medicine, Harvard Medical School, Boston, MA 02115 USA; ¹⁰Division of Gastroenterology, Brigham and Women's Hospital, Boston, MA 02115 USA; ¹¹Translational Gastroenterology Unit and Department of Pediatrics, and Biomedical Research Centre, University of Oxford, Oxford, UK; ¹²Sackler School of Medicine, Tel Aviv University, Tel-Aviv, Israel; ¹³Allergy and Clinical Immunology Unit, Schneider Children's Medical Center, Petach-Tikva, Israel; ¹⁴Gene Center, LMU Munich, Munich, Germany; ¹⁵Deutsche Zentrum für Infektionsforschung (DZIF) and Deutsches Zentrum für Kinder- und Jugendgesundheit, partner site Munich, Germany; ¹⁶VEO-IBD Consortium; ¹⁷Institute of Translational Genomics, Helmholtz Zentrum München - German Research Center for Environmental Health, Ingolstädter Landstraße 1, 85764 Neuherberg, Germany. *Contributed equally. #Corresponding author: Daniel Kotlarz, Email: daniel.kotlarz@med.uni-muenchen.de

Methods and materials

Patient

Written informed consent was acquired from the patients, first-degree relatives, and healthy volunteers upon collection of peripheral blood. This study was approved by the institutional review boards of LMU Munich and the conduction conforms to current ethical and legal frameworks.

Whole exome sequencing and Sanger sequencing

Whole exome sequencing was performed at the Dr. von Hauner Children's Hospital NGS facility. Genomic DNA was isolated from whole blood using QIAamp DNA Blood Mini Kit (Qiagen). The SureSelect XT Human All Exon V6+UTR kit (Agilent Technologies) was used to generate whole-exome libraries. Libraries were barcoded and then sequenced with NextSeq 500 platform (Illumina). Bioinformatic analysis was conducted using Burrows-Wheeler Aligner (BWA 0.7.15), Genome Analysis ToolKit (GATK 3.6) and Variant Effect Predictor (VEP 89). The in house and public databases such as ExAC, GnomAD and GME were used for frequency filtering. Sanger sequencing was performed using genome DNA from the patient and informative family members to confirm potential causative variants. Primers for Sanger sequencing were listed in Supplementary Table 1.

CRISPR/Cas9 genome editing

To knockout LY96, sgRNA targeting the 3rd exon was selected using Benchling and subcloned into pSpCas9(BB)-2A-GFP vector (PX458, Addgene). To generate patient-specific knockin, an extra repair template was designed using Benchling. Plasmids and homologous repair template were electroporated into iPSC using Human Stem Cell Nucleofector Kit 2 (Lonza) following manufacturer's protocol. GFP-positive cells were sorted using BD Aria (BD). Single cells were expanded. Selected colonies were subjected to genotyping using primers listed in

Supplementary Table 1. After genotyping, we also selected one clone without modifications on *LY96* as control (referred to as WT2).

Culture and differentiation of iPSC towards macrophages

The HMGU iPSCs were kindly provided by Helmholtz Center Munich and cultured under previously described conditions (1). Briefly, iPSCs were cultured in Matrigel Matrix- or Geltrex Matrix-coated (Corning Life Sciences and Thermo Fisher Scientific) cell culture dishes with mTeSR plus medium (StemCell technologies). Cells were passaged by collagenase IV (StemCell technologies). To differentiate iPSC into macrophages, cells were cultured with BMP4, CHIR990212, VEGF (StemCell technologies) for two days, followed by VEGF, SCF, bFGF, and SB431542 (StemCell technologies) for two days, SCF, IL-3, TPO, Flt3, and VEGF (Peprotech) for two days, and M-CSF (StemCell technologies) was added for another 6 days to reach hematopoietic stage. Cells were then cultured with GM-CSF, M-CSF, and Flt3 (StemCell technologies) to reach monocytic lineage. CD14 positive cells were enriched using EasySep human CD14 positive selection kit II (StemCell technologies) and further cultured with M-CSF for 7 days to generate macrophages.

Immunophenotyping

Blood samples from patients, parents and healthy controls were washed with PBS (Gibco) and stained with antibodies (Supplementary Table 2) in BD Brilliant stain buffer (BD Biosciences). Chemokine receptors were stained at 37 °C and other surface antigens were stained at room temperature for 15 min. Red blood cells were then lysed using BD FACS™ Lysing solution (BD). Flow cytometry acquisition was conducted on the LSRFortessa™ flow cytometer (BD) and data analysis was done using Flowjo V10.

Cloning and N-glycosidases treatment

WT *LY96* and mutant *LY96* with patient-specific mutation (c.347-349delCAA) have been amplified from healthy donor and patient cDNA using primers incorporating C-terminal flag tag sequence. The WT/mutant *LY96* fused with C-terminal flag-tagged constructs were cloned into pRRL vector. The constructs were transfected into HEK293T cells using Lipofectamine 2000TM (Thermo Fisher Scientific) according to manufacture's protocol. Transfected cells were cultured for 48 hours and lysed in cell lysis buffer (Cell Signaling). Equal amount of lysates were either treated with PNGase F or Endo H (NEB) for one hour or left untreated. All the samples were further subjected to immunoblotting with Flag antibody.

Immunoblotting

After treatment of LPS (200 ng/ml) or *E. coli* (MOI=10) for indicating time points, cells were trypsinized and lysed in NP40 buffer (1% NP40, 20 mM Tris-HCl, 1 mM EDTA, 10% glycerol) supplemented with protease inhibitors cocktail and 1 mM phenylmethylsulfonyl fluoride (Sigma Aldrich). Denatured protein lysates were subjected to 10% SDS-PAGE and transferred onto Amersham 0.2 μ m nitrocellulose membrane (Sigma-Aldrich), followed by immunoblotting using indicated antibodies (Supplementary Table 2). ChemiDocTM XRS+ system (Bio-Rad) and ImageLabTM (Bio-Rad) were used to detect and analyze the images.

Real-time qPCR

Macrophages derived from iPSC were treated with 200 ng/ml LPS for 16 hours or infected with *E. coli* (MOI=10), *Salmonella typhimurium* (MOI=10), or heat-killed *Listeria monocytogenes* (4×10^7 HKLM/ml) for 3 hours. Total RNA was isolated using PureLinkTM RNA Mini-Kits (Thermo Fisher Scientific), then reverse transcribed into cDNA using High-Capacity cDNA Reverse Transcription Kit (Thermo Fisher Scientific) following manufacturer's protocol. Real-time qPCR was performed using PowerUpTM SYBRTM Green Master Mix (Thermo Fisher

Scientific) and primers listed in Supplementary Table 1. KO group was used as reference to calculate relative fold change of indicated genes.

ELISA

To assess IL-1 β secretion, patient- or iPSC-derived macrophages were treated with LPS (200 ng/ml; Invivogen) \pm nigericin (6.5 μ M; Enzo Life Sciences) for 18 hours or infected with *E.coli* (MOI=10) for 3 and 6 hours. Mature IL-1 β in supernatants were assessed using the Human IL-1 β /IL-1F2 DuoSet ELISA kit (DY201, R&D Systems). OD450 was measured in duplicates by Synergy H1 microplate reader (BioTek Instrument).

Flow cytometry

Differentiated macrophages were treated with LPS (200 ng/ml) or *E.coli* (MOI=10) for indicated time. After treatment, cells were fixed with 3.7% paraformaldehyde in PBS (Santa Cruz) for 20 minutes, and stained with TLR4 antibody (PE-conjugated). Flow cytometry acquisition was done on the LSRFortessaTM flow cytometer (BD) and data analysis was performed using Flowjo V10.

Confocal microscopy

To study TLR4 endocytosis, macrophages were stimulated with LPS (200 ng/ml) for indicated time. After treatment, cells were fixed by 3.7% Paraformaldehyde in PBS (Santa Cruz) for 20 minutes, permeablized by 0.5% Nonidet P40 (Sigma-Aldrich) and blocked in 1% BSA. Cells were subsequently stained with TLR4-PE (BD), EEA1-FITC (BD), and LAMP1 antibodies (Cell Signaling Technology). To assess *Salmonella typhimurium* infection, cells were infected with MOI 10 for one hour, then incubated with lysotracker Deep Red (0.1%, Thermo Fisher Scientific) and gentamycin (50 μ g/ml, Thermo Fisher Scientific) for one hour. Cells were then fixed and permeablized as described above, and stained with LC3B antibody (Cell Signaling

134 Technology) and DAPI (Sigma Aldrich). Imaging was performed and analyzed using Zeiss
135 LSM800 (Zeiss).

136

137 **Phagocytosis assay**

138 Macrophages derived from iPSC were seeded in 35 mm μ -Dish with coverslip bottom (ibidi).
139 Cells were recorded every minute for 32 min upon treatment with pHrodo Red *E.coli*
140 bioparticles conjugate for phagocytosis (Thermo Fisher Scientific) on Zeiss LSM800 live cell
141 imaging system (Zeiss). Only particles in acidic environment (phagosomes) show bright red
142 fluorescence. Around 30 cells were recorded and analyzed for phagosome formation indicated
143 by increased red fluorescence intensity.

144

145 **Statistics**

146 Statistical analyses were performed using One-way ANOVA with Dunnett's correction or
147 Friedman test. Each circle symbol indicates one independent experiment. P values were shown
148 by comparison to WT from the same treatment. P values < 0.05 were considered as statistically
149 significant.

150 **Supplementary tables**

151 **Table S1.** List of antibodies.

Antibodies	Company	Cat no.
Phospho-NF-κB-p65 (S536)	Cell Signaling	3033s
NF-κB-p65	Cell Signaling	8242s
phospho-p38 MAPK (T180/Y182)	Cell Signaling	4511s
p38 MAPK	Cell Signaling	9212s
phospho-p44/42 MAPK (T202/Y204)	Cell Signaling	4370s
p44/42 MAPK	Cell Signaling	9102s
GAPDH	Proteintech	HRP-60004
TLR4-PE	BD Biosciences	564215
CD14	BD Biosciences	555397
EEA1-FITC	BD Biosciences	15876069
LAMP1	Cell signaling	9091s
NLRP3	Cell signaling	13158s
IL-1beta	R&D	AF-201-NA
caspase-1	Abcam	ab179515
Beta-Actin	Santa Cruz	sc-47778HRP

152

153

154 **Table S2.** List of primers and guide RNAs.

Primers	Sequence
genotyping	
<i>LY96_KI_F</i>	GCATATTAGCACTAGCTTGTTTCATCG
<i>LY96_KI_R</i>	CGTCTCTTCCAAAAGTACAAAACATTAG
<i>LY96_KO_F</i>	GCACAGGGCCCCCTTTTAACTAT
<i>LY96_KO_R</i>	CAAGGAGGAACATAAAGGCAGAAG
qPCR	
<i>LY96_qF</i>	ATTTGCCGAGGATCTGATGACG
<i>LY96_qR</i>	GGCTCCCAGAAATAGCTTCAAC
<i>IL6_qF</i>	AAGCGCCTTCGGTCCAGTT
<i>IL6_qR</i>	CATGTCTCCTTTCTCAGGGCT
<i>IL1b_qF</i>	CAAGCTGAGGAAGATGCTGGTT
<i>IL1b_qR</i>	ATCGTGCACATAAGCCTCGTTATCC
<i>TNF_qF</i>	TGCACTTTGGAGTGATCGGC
<i>TNF_qR</i>	ACTCGGGGTTTCGAGAAGATG
<i>IL10_qF</i>	CAACCTGCCTAACATGCTTCGAGAT
<i>IL10_qR</i>	CCTCCAGCAAGGACTCCTTTAACAAC
<i>GAPDH_qF</i>	GTCTCCTCTGACTTCAACAGCG
<i>GAPDH_qR</i>	ACCACCCTGTTGCTGTAGCCAA
sgRNA	
guide1 KO <i>LY96</i> fw	CACCGTCTACTATTTGAGGGCCTAA
guide1 KO <i>LY96</i> rv	AAACTTAGGCCCTCAAATAGTAGAC
guide2 KO <i>LY96</i> fw	CACCGTTTTGCAGAGCTCTGAAGGG
guide2 KO <i>LY96</i> rv	AAACCCCTTCAGAGCTCTGCAAAAC
<i>LY96_KI_sgF</i>	CACCGAACAATATCATTCTCCTTCA
<i>LY96_KI_sgR</i>	AAACTGAAGGAGAATGATATTGTTC

155

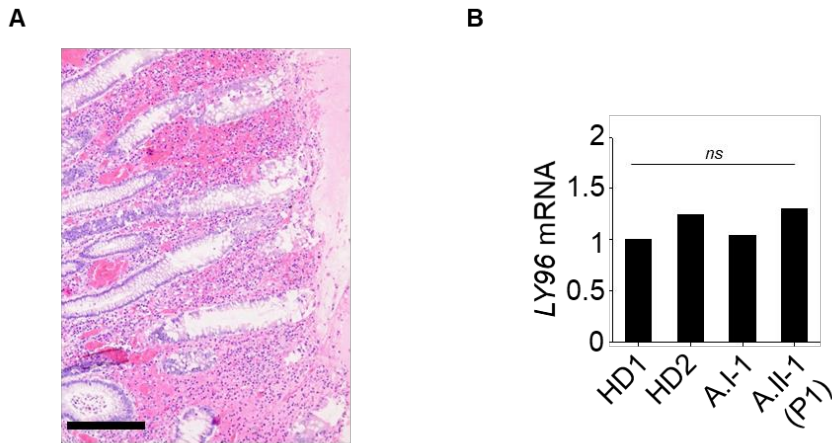
156

Supplementary Figures

Supplementary Figure S1. (A) Higher magnification of histology reveals moderate colitis.

Scale bar is 250 μ m. Related to Fig.1C **(B)** RNA expression of *LY96* in EBV-LCL from healthy

controls, father (A.I-1) and patient (A.II-1).

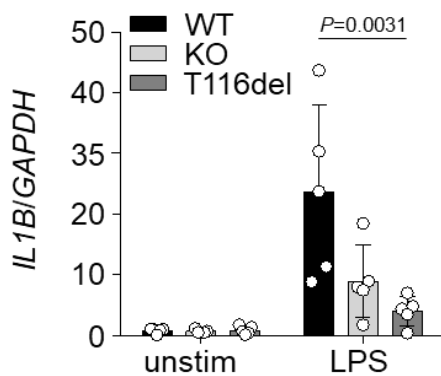


Supplementary Figure 1

Supplementary Figure S2. Real time-qPCR confirmed reduced production of IL-1 β upon

stimulation with LPS and nigericin in iPSC-derived macrophages with KO of MD2 or KI of

the mutation p.Thr116del. Related to Fig. 2C.



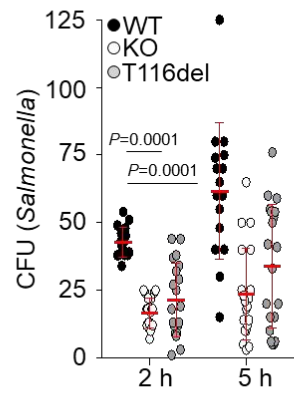
Supplementary Figure 2

Supplementary Figure S3. (A) Gentamycin protection assay revealed less colony formation

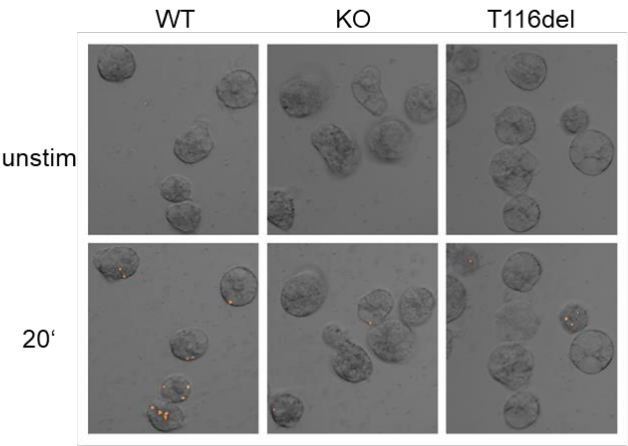
units in MD2-deficient macrophages after infection with *Salmonella typhimurium*. **(B)**

168 Representative pictures at 0 min and 20 min from live cell imaging with pHrodo Red *E.coli*
169 bioparticles suggested delayed phagocytosis. Related to Fig. 3E.

A



B



Supplementary Figure 3

172 **References**

- 173 1. Kunze C, Borner K, Kienle E, Orschmann T, Rusha E, Schneider M, et al. Synthetic
174 AAV/CRISPR vectors for blocking HIV-1 expression in persistently infected astrocytes. *Glia*.
175 2018;66(2):413-27.
176

